



Efficient and selective conversion of methyl lactate to acrylic acid using $\text{Ca}_3(\text{PO}_4)_2\text{-Ca}_2(\text{P}_2\text{O}_7)$ composite catalysts

Ju Hyeong Hong, Jong-Min Lee, Hyungrok Kim, Young Kyu Hwang, Jong-San Chang*, Shiva B. Halligudi*, Yo-Han Han*

Catalysis Center for Molecular Engineering, Korea Research Institute of Chemical Technology (KRICT), P.O. Box 107, Yuseong, Daejeon 305-600, South Korea

ARTICLE INFO

Article history:

Received 20 October 2010

Received in revised form 10 February 2011

Accepted 15 February 2011

Available online 21 February 2011

Keywords:

Methyl lactate

Acrylic acid

Methyl acrylate

$\text{Ca}_3(\text{PO}_4)_2$

$\text{Ca}_2(\text{P}_2\text{O}_7)$

ABSTRACT

Calcium phosphate $\text{Ca}_3(\text{PO}_4)_2$ and calcium pyrophosphate $\text{Ca}_2(\text{P}_2\text{O}_7)$ composite catalysts of different weight ratios were prepared by a slurry-mixing method. These composite catalysts were calcined at 500 °C in air and characterized by N_2 sorption for specific surface area by XRD for crystal phases and by TPD- NH_3 (acidity), TPD- CO_2 (basicity) and SEM for morphological features. All the $\text{Ca}_3(\text{PO}_4)_2\text{-Ca}_2(\text{P}_2\text{O}_7)$ composite catalysts were found to be active in the vapor phase conversion of methyl lactate (ML) to give mainly acrylic acid (AA) and methyl acrylate (MA) as products. The catalyst $\text{Ca}_3(\text{PO}_4)_2\text{-Ca}_2(\text{P}_2\text{O}_7)$ of 50:50 wt% ratio was the most efficient and selective catalyst in the conversion of ML, which gave 91% conversion of ML with selectivity for AA (75%) and MA (5%) together (80%) under optimized reaction conditions. The higher conversion of ML and formation of AA by $\text{Ca}_3(\text{PO}_4)_2\text{-Ca}_2(\text{P}_2\text{O}_7)$ [50:50 wt%] composite catalyst has been attributed to moderate acid–base strength regulated with surface properties.

© 2011 Elsevier B.V. All rights reserved.

1. Introduction

The petroleum energy crisis has been triggered in recent years by the increase in demand and higher price of petroleum based chemicals. This has necessitated the search for alternate sources for producing valuable chemicals and fuels. The utilization of renewable raw material is a recent trend in biorefinery research for this purpose. However, there are limited options for renewable sources to meet the above demand. The economic feasibility of the new processes based on available alternate raw materials has to be worked out for a sustainable future for the chemical industry.

Among the alternate sources, biomass has been specially utilized for producing chemicals and fuels in combination with biotechnology and chemical catalysis routes. Biomass of agriculture, forestry and industrial wastes could be converted to chemicals through fermentation and thermo-chemical processes based on the heterogeneous catalysis. Given the current robust forces driving sustainable chemical production and available biomass conversion technologies, biomass-based routes are expected to make a significant impact on the chemical industry for producing bulk chemicals

in coming 10 years [1–10]. One such target is the efficient conversion of biomass derived lactic acid (LA)/or methyl lactate (ML) to acrylic acid (AA), which is expected to open a new field of chemical industry thanks to the substitution of various petroleum based commercial acrylates.

The biomass based AA has been prepared by LA or alkyl lactates dehydration via fermentation and/or chemical conversion routes using novel recombinant microorganism and chemical catalysis [11]. There are a few reports in the literature dealing with ML dehydration catalyst systems resulting in high yields of AA. These catalysts include calcium phosphate supported on silica, sodium salts of group IV and group V oxides, alkali metal salts on silica and KNaY-zeolite [12–18]. Recently, it is reported that 12 wt% NaH_2PO_4 on SiO_2 catalyst was active in the conversion of ML (78.9%) at 340 °C with WHSV, 6.9s^{-1} and this yielded poor selectivity of 39.8% for AA and MA together. The above catalyst system favored decarbonylation and dehydration to give large amounts of acetaldehyde probably due to strong acidity [19].

We have also studied phosphate type catalyst systems of the dispersed $\text{Ca}_3(\text{PO}_4)_2$ on SiO_2 in our laboratory, such system gave fairly high ML conversion (73%) and high AA and MA selectivity (77%) together [12]. In continuation of our work on ML conversion, we report here our new findings wherein $\text{Ca}_3(\text{PO}_4)_2\text{-Ca}_2(\text{P}_2\text{O}_7)$ composite catalysts have been applied for the efficient conversion of ML to give AA under vapor phase reaction conditions.

* Corresponding authors. Tel.: +82 42 860 7565; fax: +82 42 860 7676.

E-mail addresses: jschang@kRICT.re.kr (J.-S. Chang), sb.halligudi123@yahoo.co.in (S.B. Halligudi), yhhan@kRICT.re.kr (Y.-H. Han).

2. Materials and methods

2.1. Materials

ML, ethyl lactate (EL) and lactic acid (LA) supplied by Aldrich were used as received in the catalytic reactions. Acetaldehyde, methyl acrylate, methoxy methyl propionate, acetone, propionic acid, hydroquinone, and AA were obtained from Aldrich for gas chromatographic analysis reference materials. Sodium pyrophosphate ($\text{Na}_4\text{P}_2\text{O}_7$), sodium phosphate ($\text{Na}_3\text{PO}_4 \cdot 12\text{H}_2\text{O}$) and CaCl_2 (hydrous) were supplied by Daejung Chemicals and Metals. Deionized water (DW) was used in all the catalyst preparations.

2.2. Methods

2.2.1. Preparation of $\text{Ca}_3(\text{PO}_4)_2$ – $\text{Ca}_2(\text{P}_2\text{O}_7)$ composite catalysts

A series of $\text{Ca}_3(\text{PO}_4)_2$ – $\text{Ca}_2(\text{P}_2\text{O}_7)$ composite catalysts with different weight ratios, which varied in the range 30–80 wt%, were prepared by slurry mixing of two components in water and heat treatment of the isolated $\text{Ca}_3(\text{PO}_4)_2$ – $\text{Ca}_2(\text{P}_2\text{O}_7)$ powder mixture. The slurries of the two components, $\text{Ca}_3(\text{PO}_4)_2$ and $\text{Ca}_2(\text{P}_2\text{O}_7)$ were prepared with $\text{CaCl}_2 \cdot 2\text{H}_2\text{O}$ solution via precipitation from the aqueous solutions of $\text{Na}_4\text{P}_2\text{O}_7$ and $\text{Na}_3\text{PO}_4 \cdot 12\text{H}_2\text{O}$, respectively.

- $\text{Ca}_3(\text{PO}_4)_2$ slurry: $\text{Ca}_3(\text{PO}_4)_2$ slurry was prepared by mixing a solution of 38.01 g of $\text{Na}_3\text{PO}_4 \cdot 12\text{H}_2\text{O}$ (0.1 mol, 98%, in 250 ml DW) and a solution of $\text{CaCl}_2 \cdot 2\text{H}_2\text{O}$, 23.52 g (0.16 mol, in 100 ml DW) by slow addition of 7 ml/min of $\text{CaCl}_2 \cdot 2\text{H}_2\text{O}$ solution with continuous stirring at 60 °C for 1 h to result in a white powdery slurry.
- $\text{Ca}_2(\text{P}_2\text{O}_7)$ slurry: $\text{Ca}_2(\text{P}_2\text{O}_7)$ slurry was prepared by mixing a solution of 32.44 g of $\text{Na}_4\text{P}_2\text{O}_7$ (0.122 mol, prepared in 250 ml of DW heating at 50 °C) and a solution of 39.46 g $\text{CaCl}_2 \cdot 2\text{H}_2\text{O}$ (0.268 mol in 100 ml DW) by slow addition of 7 ml/min of $\text{CaCl}_2 \cdot 2\text{H}_2\text{O}$ solution with continuous stirring at room temperature for 1 h to get a white powdery slurry.
- Slurry mixing, isolation and heat treatment: the $\text{Ca}_3(\text{PO}_4)_2$ slurry (a) and the $\text{Ca}_2(\text{P}_2\text{O}_7)$ slurry (b) were filtered and each dispersed in 350 ml of DW twice and filtered again to get $\text{Ca}_3(\text{PO}_4)_2$ and $\text{Ca}_2(\text{P}_2\text{O}_7)$ cakes, respectively. Determined ratios of the two cakes were dispersed in 500 ml of DW and physically mixed by continuous stirring at room temperature for 1 h. The mixed slurry was filtered and dried at 80 °C in air circulating oven for 6 h and then the resulting white powder was pressed at 100 kgf/cm² to get tablets. The particles of $\text{Ca}_3(\text{PO}_4)_2$ – $\text{Ca}_2(\text{P}_2\text{O}_7)$ of 0.45–0.85 mm diameter sizes were collected by sieving the crushed tablets. These $\text{Ca}_3(\text{PO}_4)_2$ – $\text{Ca}_2(\text{P}_2\text{O}_7)$ composite particles were calcined at 500 °C in air for 6 h to result in the composite catalysts.

2.3. Catalysts characterization

X-ray diffraction properties were measured using a Brucker D8 ADVANCE X-ray diffractometer with Cu K α monochromatized radiation source, operated at 40 kV, 30 mA and a scanning speed of 5°/min. BET surface area was determined from N₂

adsorption–desorption isotherms using an Autopore IV 9500 Series from Micrometrics. Temperature programmed desorption (TPD) was performed on AutoChem II 2920 Chemisorptions Analyzer to get the acidic and basic sites of catalysts. The particle size and the morphology of the catalysts were examined using a scanning electron microscope (SEM, JEOL JSM-840A).

2.4. Experimental procedure

The dehydration reactions of ML were conducted in a Pyrex glass tubular down flow micro-reactor of 35 cm in length and 8 mm inner diameter (Scheme 1). Catalyst (6 ml = 4 g) of 0.45–0.85 mm diameter size was charged on the glass wool packed bed in the middle section of the reactor. Liquid feed, aqueous 50 wt% ml solution, was injected into the top of the reactor by a syringe pump along with N₂ carrier gas flow at the desired reaction temperature. Before the reactant feed, the catalyst bed was pre-heated at 400 °C in the reactor with N₂ flow and then maintained at the test temperature for 1 h. The reaction products of ML dehydration were condensed in the cold trap after 24 h continuous reaction and then analyzed using GC (HP5890) equipped with DB-WAX capillary column and an FID detector. Also, EL and LA conversions were performed to figure out the reactant dependency of the composite catalyst system for getting AA.

3. Results and discussion

3.1. Physical characteristics of $\text{Ca}_3(\text{PO}_4)_2$ and $\text{Ca}_2(\text{P}_2\text{O}_7)$

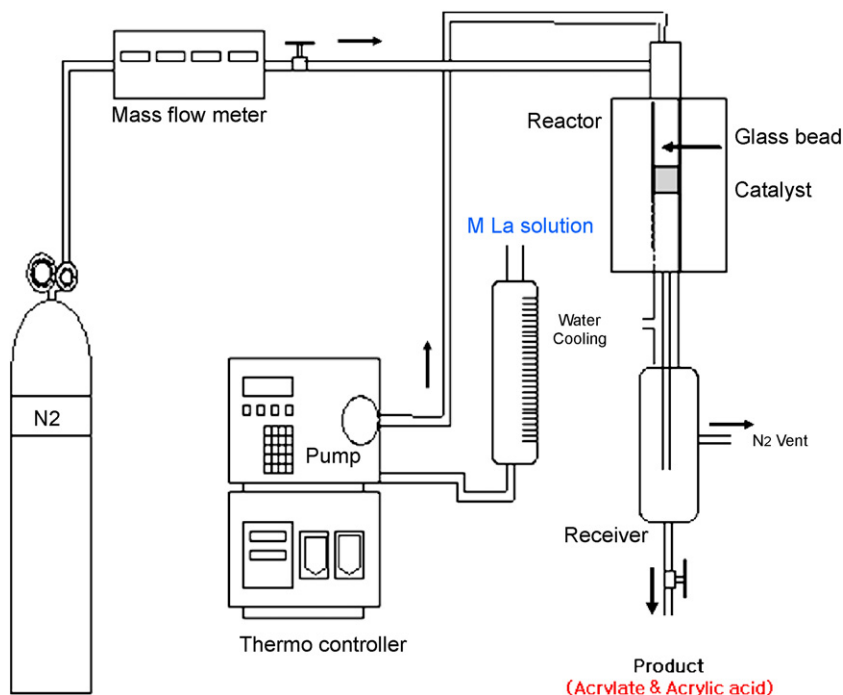
It is known that $\text{Ca}_3(\text{PO}_4)_2$ upon ignition changes to crystalline α - or β -tricalcium phosphates (TCP) and no P₂O₅ component as acid phosphate are observed [20]. This means that $\text{Ca}_3(\text{PO}_4)_2$ is very stable against heat stress. When a hydrated form of $\text{Ca}_3(\text{PO}_4)_2$ is calcined at 570 °C for 5 h, it changed to partially dehydrated state without losing its chemical identity. However, it is also reported that $\text{Ca}_3(\text{PO}_4)_2$ at 500 °C, exists in its partially hydrated form and transforms slowly into $\text{Ca}_2(\text{P}_2\text{O}_7)$ by heat treatment. The effect of heat treatment on the physicochemical property changes of $\text{Ca}_3(\text{PO}_4)_2$ – $\text{Ca}_2(\text{P}_2\text{O}_7)$ mixed phases is not known.

3.2. Physical properties of the composite catalysts

It is seen from the results presented in Table 1 that $\text{Ca}_3(\text{PO}_4)_2$ and $\text{Ca}_2(\text{P}_2\text{O}_7)$ have low specific surface areas of 37.4 and 2.4 m²/g, respectively, with the average pore size range 26–45 nm, indicating the highly porous nature of the materials. The specific surface areas of $\text{Ca}_3(\text{PO}_4)_2$ – $\text{Ca}_2(\text{P}_2\text{O}_7)$ composite catalysts lie in between the two pure components. Similarly, the pore volume of $\text{Ca}_3(\text{PO}_4)_2$ – $\text{Ca}_2(\text{P}_2\text{O}_7)$ composite catalysts decreased with increase in $\text{Ca}_2(\text{P}_2\text{O}_7)$ contents (0.32–0.03 cm³/g), which suggests that the composite material is mainly a physical mixture of $\text{Ca}_3(\text{PO}_4)_2$ and $\text{Ca}_2(\text{P}_2\text{O}_7)$ components in the bulk. However, the total amounts of acidity and basicity of the composite materials show different deviation from the linear type trend of other physical property changes with the composition ratios. There exists relatively low acidity and basicity with 50:50 wt% $\text{Ca}_3(\text{PO}_4)_2$ – $\text{Ca}_2(\text{P}_2\text{O}_7)$ composite material,

Table 1
Physicochemical properties of $\text{Ca}_3(\text{PO}_4)_2$ – $\text{Ca}_2(\text{P}_2\text{O}_7)$ composite catalysts calcined at 500 °C.

Catalyst composition (wt%)	Surface area (m ² /g)	Pore volume (cm ³ /g)	Pore size (nm)	Acidity (mmol NH ₃ /g)	Basicity (mmol CO ₂ /g)
1) $\text{Ca}_3(\text{PO}_4)_2$	37.4	0.32	34	0.30	0.18
2) $\text{Ca}_3(\text{PO}_4)_2$ – $\text{Ca}_2(\text{P}_2\text{O}_7)$ [70:30]	18.8	0.14	30	0.32	0.16
3) $\text{Ca}_3(\text{PO}_4)_2$ – $\text{Ca}_2(\text{P}_2\text{O}_7)$ [50:50]	12.4	0.08	26	0.13	0.10
4) $\text{Ca}_3(\text{PO}_4)_2$ – $\text{Ca}_2(\text{P}_2\text{O}_7)$ [20:80]	2.5	0.03	40	0.18	0.19
5) $\text{Ca}_2(\text{P}_2\text{O}_7)$	2.4	0.03	44	0.16	0.22



Scheme 1. Experimental set-up for the ML conversion.

which reflected the changes that occurred in the surface properties during calcination. However, the role of Brønsted and Lewis acidities of the composite materials has not been evaluated in our studies to assess their effects on ML conversions and product selectivities in the reaction.

XRD patterns of $\text{Ca}_3(\text{PO}_4)_2$ - $\text{Ca}_2(\text{P}_2\text{O}_7)$ composite catalysts of different wt% ratios for fresh (calcined at 500°C) and used catalysts are presented in Figs. 1 and 2. These figures show that fresh as well as used catalysts have distinct diffraction patterns of $\text{Ca}_3(\text{PO}_4)_2$ phase and $\text{Ca}_2(\text{P}_2\text{O}_7)$ phase [19]. When $\text{Ca}_2(\text{P}_2\text{O}_7)$ component increases in fresh and used composite catalysts, the diffraction peak intensity of $\text{Ca}_2(\text{P}_2\text{O}_7)$ phase increased. Thus, in the diffraction patterns of the fresh and used catalyst systems, no significant enhancement of the diffraction peaks of $\text{Ca}_2(\text{P}_2\text{O}_7)$ phase, which might be a result of the possible extra transformation of $\text{Ca}_3(\text{PO}_4)_2$ phase during the high temperature calcination are not observed. The absence of significant enhancement in $\text{Ca}_2(\text{P}_2\text{O}_7)$

diffraction peaks suggests that there is no phase change in the bulk of $\text{Ca}_3(\text{PO}_4)_2$ particles.

A typical example of the $\text{Ca}_3(\text{PO}_4)_2$ - $\text{Ca}_2(\text{P}_2\text{O}_7)$ catalyst system, SEM images of $\text{Ca}_3(\text{PO}_4)_2$ - $\text{Ca}_2(\text{P}_2\text{O}_7)$ [50:50 wt%] of fresh and used catalysts are presented in Fig. 3. It is seen that the fresh and used catalysts show extended lath shape (slender elongated form) particles, which are characteristics of both $\text{Ca}_3(\text{PO}_4)_2$ and $\text{Ca}_2(\text{P}_2\text{O}_7)$ components. However, definite shape and particle sizes are not quantified in our studies. SEM observations suggest that the used catalyst has retained its morphology after 24 h in ML conversion reaction, which is supported by XRD diffraction patterns.

3.3. Acidity–basicity of the calcined $\text{Ca}_3(\text{PO}_4)_2$ - $\text{Ca}_2(\text{P}_2\text{O}_7)$ composite catalysts

The acidity and basicity data estimated by TPD- NH_3 (acidity) and TPD- CO_2 (basicity) are listed in Table 1. Also, the TPD patterns of the

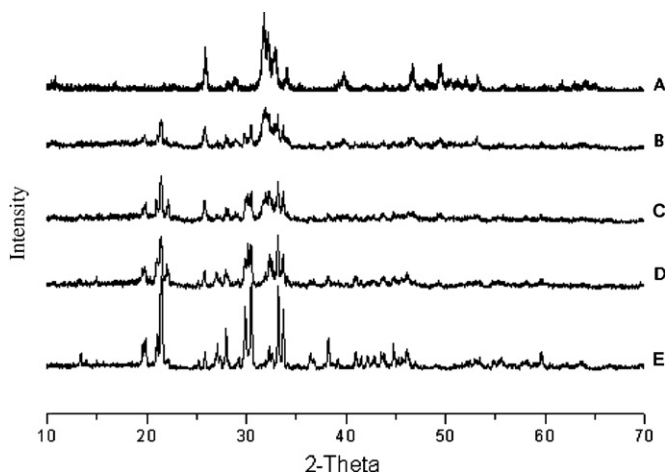


Fig. 1. XRD patterns of fresh composite catalysts calcined at 500°C : (A) $\text{Ca}_3(\text{PO}_4)_2$; (B) $\text{Ca}_3(\text{PO}_4)_2$ - $\text{Ca}_2(\text{P}_2\text{O}_7)$ [70:30 wt%]; (C) $\text{Ca}_3(\text{PO}_4)_2$ - $\text{Ca}_2(\text{P}_2\text{O}_7)$ [50:50 wt%]; (D) $\text{Ca}_3(\text{PO}_4)_2$ - $\text{Ca}_2(\text{P}_2\text{O}_7)$ [20:80 wt%]; (E) $\text{Ca}_2(\text{P}_2\text{O}_7)$.

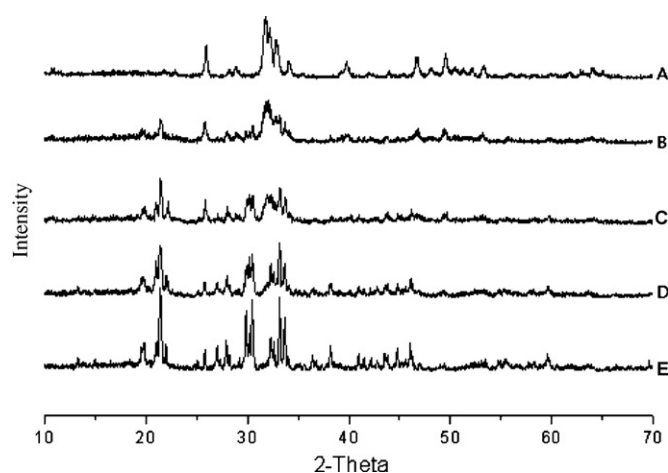


Fig. 2. XRD pattern of used composite catalysts in ML conversion: (A) $\text{Ca}_3(\text{PO}_4)_2$; (B) $\text{Ca}_3(\text{PO}_4)_2$ - $\text{Ca}_2(\text{P}_2\text{O}_7)$ [70:30 wt%]; (C) $\text{Ca}_3(\text{PO}_4)_2$ - $\text{Ca}_2(\text{P}_2\text{O}_7)$ [50:50 wt%]; (D) $\text{Ca}_3(\text{PO}_4)_2$ - $\text{Ca}_2(\text{P}_2\text{O}_7)$ [20:80 wt%]; (E) $\text{Ca}_2(\text{P}_2\text{O}_7)$.

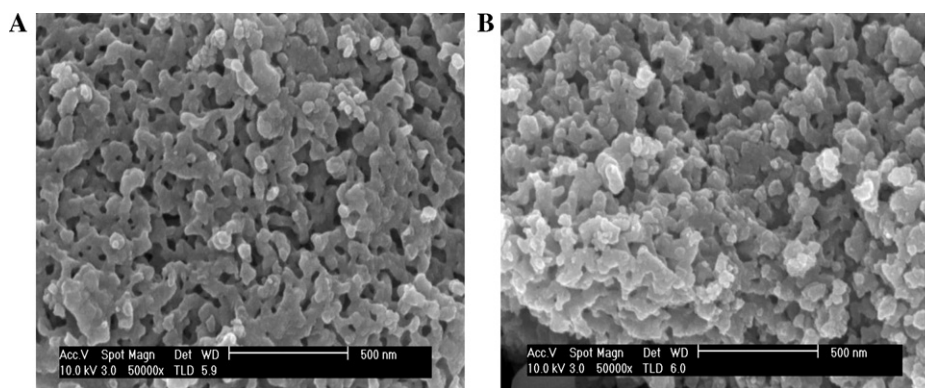


Fig. 3. SEM images of $\text{Ca}_3(\text{PO}_4)_2\text{-Ca}_2(\text{P}_2\text{O}_7)$ [50:50 wt%] composite catalyst: (A) fresh catalyst calcined at 500 °C, (B) used catalyst.

fresh and used composite catalysts are compared in Figs. 4 and 5, respectively. As already noticed (Table 1), the pattern of acidity and basicity changes in the $\text{Ca}_3(\text{PO}_4)_2\text{-Ca}_2(\text{P}_2\text{O}_7)$ composite catalysts does not follow an average relationship with composition variation. Especially for the 50:50 wt% $\text{Ca}_3(\text{PO}_4)_2\text{-Ca}_2(\text{P}_2\text{O}_7)$ composite catalyst, abrupt decreases in acidity and basicity values (0.133 mmol NH_3 and 0.096 mmol CO_2) are observed which are significantly lower than those of both ends. The TPD patterns (Figs. 4 and 5) also describe the definite changes of acid–base strength distributions in the $\text{Ca}_3(\text{PO}_4)_2\text{-Ca}_2(\text{P}_2\text{O}_7)$ composite catalyst system. In the composite catalysts, the desorption peaks correspond to low and high strength of acidic and basic sites, which are moved toward modulated positions and diffused middle strength peaks generally appeared, probably due to the surface property modification during the heat treatment. It is not clear at this moment how the acid–base properties of the composite catalysts are affected by mixing the two components and after heat treatment, even without significant changes of other bulk physical properties.

3.4. Conversion of methyl lactate (ML)

The catalytic activities of the $\text{Ca}_3(\text{PO}_4)_2\text{-Ca}_2(\text{P}_2\text{O}_7)$ composite catalysts in ML conversions are listed in Table 2. The conversions of ML by $\text{Ca}_3(\text{PO}_4)_2\text{-Ca}_2(\text{P}_2\text{O}_7)$ composite catalysts over the con-

trolled reaction conditions [ML: 50% in water, flow rate: 2.1 ml h^{-1} , LHSV = 0.175, N_2 flow rate: 15 ml min^{-1} , catalyst: 6 ml (4.0 g), TOS: 27 h, temp.: 390 °C] gave mainly AA, MA, acetaldehyde, propionic acid and other small amounts of gaseous by-products such as carbon monoxide and hydrogen. It is to be noticed that $\text{Ca}_3(\text{PO}_4)_2$ (pure) gave 98% conversion of ML with a selectivity AA (39%) and MA (20%) along with other products, while $\text{Ca}_2(\text{P}_2\text{O}_7)$ (pure) gave 72% ML conversion with AA (65%) and MA (1%). One can see that the $\text{Ca}_3(\text{PO}_4)_2\text{-Ca}_2(\text{P}_2\text{O}_7)$ composite catalyst system follows the expected decreasing pattern in the ML conversions due to the changes in acid–base strength with increase in $\text{Ca}_2(\text{P}_2\text{O}_7)$ amounts. However, the selectivity for AA and MA reached the highest values, AA (75%) and MA (5%) together 80% at 50:50 wt% $\text{Ca}_3(\text{PO}_4)_2\text{-Ca}_2(\text{P}_2\text{O}_7)$ catalyst composition at ML conversion (91%). The objective of this investigation was to achieve higher selectivities for AA and MA at reasonably higher ML conversions. The higher ML conversion (91%) and product selectivities for AA and MA together (80%) by $\text{Ca}_3(\text{PO}_4)_2\text{-Ca}_2(\text{P}_2\text{O}_7)$ [50:50 wt%] composite catalyst has been attributed to the changes in the surface acid–base strength.

Based on the product distribution and the formation of carbon monoxide and hydrogen (0.5–2% selectivity range) in the conversion of ML catalyzed by $\text{Ca}_3(\text{PO}_4)_2\text{-Ca}_2(\text{P}_2\text{O}_7)$ catalyst system at high temperature vapor phase reaction conditions, possible reaction pathways suggested are shown in Scheme 2. As seen from

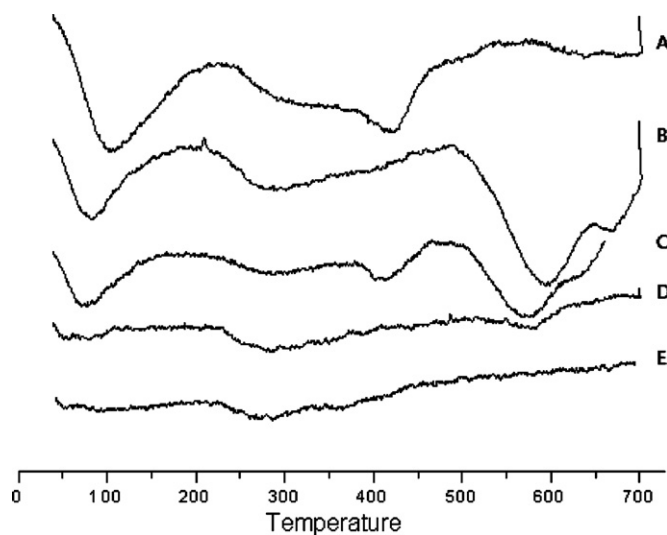


Fig. 4. TPD- NH_3 patterns of $\text{Ca}_3(\text{PO}_4)_2\text{-Ca}_2(\text{P}_2\text{O}_7)$ composite catalysts calcined at 500 °C: (A) $\text{Ca}_3(\text{PO}_4)_2$; (B) $\text{Ca}_3(\text{PO}_4)_2\text{-Ca}_2(\text{P}_2\text{O}_7)$ [70:30 wt%]; (C) $\text{Ca}_3(\text{PO}_4)_2\text{-Ca}_2(\text{P}_2\text{O}_7)$ [50:50 wt%]; (D) $\text{Ca}_3(\text{PO}_4)_2\text{-Ca}_2(\text{P}_2\text{O}_7)$ [20:80 wt%]; (E) $\text{Ca}_2(\text{P}_2\text{O}_7)$.

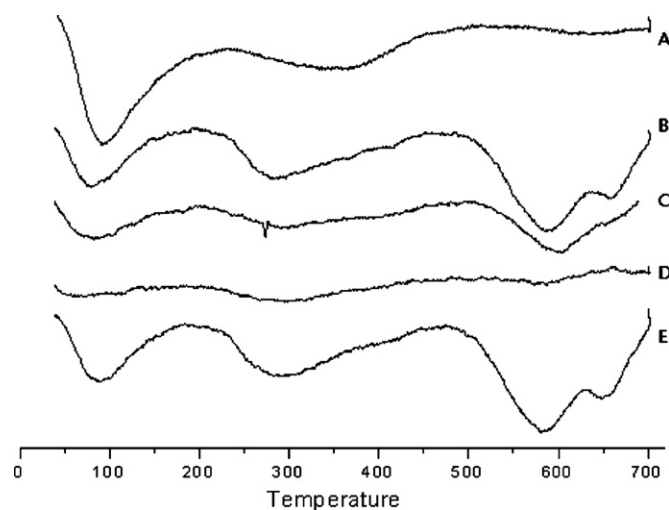


Fig. 5. TPD- CO_2 patterns of $\text{Ca}_3(\text{PO}_4)_2\text{-Ca}_2(\text{P}_2\text{O}_7)$ composite catalysts calcined at 500 °C: (A) $\text{Ca}_3(\text{PO}_4)_2$; (B) $\text{Ca}_3(\text{PO}_4)_2\text{-Ca}_2(\text{P}_2\text{O}_7)$ [70:30 wt%]; (C) $\text{Ca}_3(\text{PO}_4)_2\text{-Ca}_2(\text{P}_2\text{O}_7)$ [50:50 wt%]; (D) $\text{Ca}_3(\text{PO}_4)_2\text{-Ca}_2(\text{P}_2\text{O}_7)$ [20:80 wt%]; (E) $\text{Ca}_2(\text{P}_2\text{O}_7)$.

Table 2
ML conversions using $\text{Ca}_3(\text{PO}_4)_2\text{-Ca}_2(\text{P}_2\text{O}_7)$ composite catalysts at 390 °C.

$\text{Ca}_3(\text{PO}_4)_2\text{-Ca}_2(\text{P}_2\text{O}_7)$ (wt%)	Conv. (%)	Product selectivity (%)				
		Acrylic acid	Methyl acrylate	Acetal-dehyde	Propionic acid	Others ^a
100:0	98	39	20	31	7	3
70:30	99	61	7	18	11	3
50:50	91	75	5	14	4	2
20:80	70	66	3	16	10	5
0:100	72	65	1	17	14	3

Reaction conditions: ML feedstock: 50% in water, ML flow rate: 2.1 ml h⁻¹, LHSV = 0.175, N₂ flow rate: 15 ml min⁻¹, catalyst: 6 ml (4.0 g), TOS: 27 h, temp.: 390 °C (663 K).

^a Others contain 0.5–2% of carbon monoxide which are roughly proportional to acetaldehyde formations and the rest are methoxy methyl propionate, acetol, D-lactide and hydrogen.

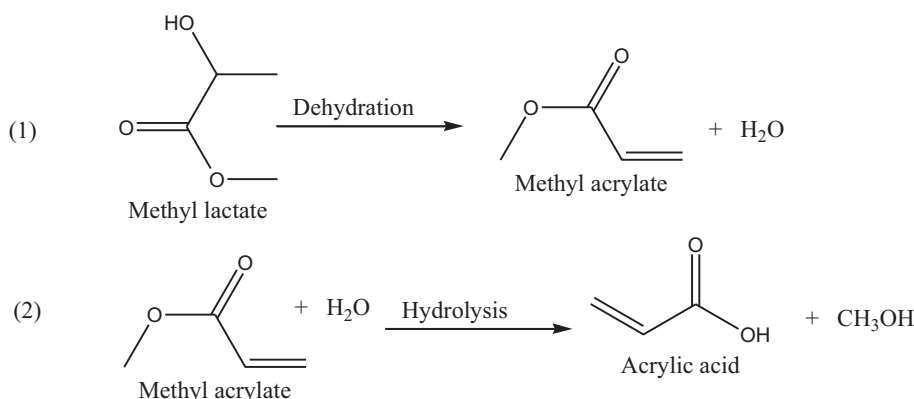
Scheme 2, the main reactions of ML conversion to AA are dehydration of ML and hydrolysis of MA to AA, while side reactions are decomposition of ML to give propionic acid, acetaldehyde carbon monoxide and hydrogen, which also have been reported in the literature [19,21]. The formation of propionic acid and acetaldehyde from AA and MA might be considered, together with ML decomposition pathways, as parallel side reactions. This needs to be checked through some controlling experiments that are described below.

To check the formation of propionic acid and acetaldehyde, we conducted some experiments with AA as a feed under the reaction conditions of ML decomposition. It was found that the AA conversion observed was very low (2%) and the selectivity for propionic acid was low, while the selectivity for acetaldehyde was high. As the AA conversion is too low (2%), the conversion of AA to propionic acid and acetaldehyde has been ruled out in **Scheme 2**. Similarly, when methyl acrylate (MA) was used as a feed, the selectivities for AA, propionic acid and acetaldehyde were not changed and were nearly the same as the values reported for ML conversions (**Tables 2–5**). Hence, as shown in **Scheme 2**, the side reaction pathways shown are more appropriate and confirm the formation of acetaldehyde,

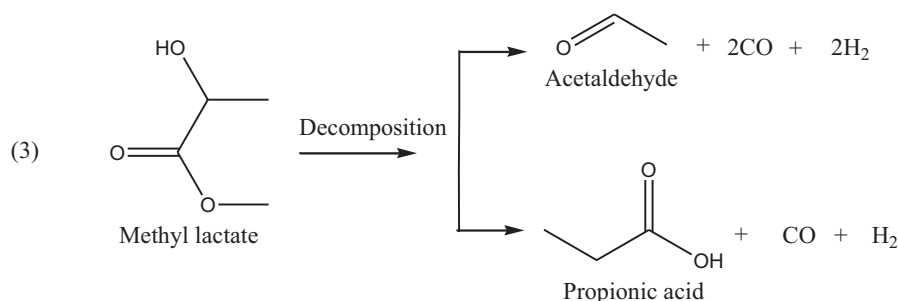
propionic acid, carbon monoxide and hydrogen from ML or MA conversions only.

The expected achievements in this investigation are higher ML conversion and higher selectivity for AA and MA via efficient dehydration followed by hydrolysis. Under the vapor phase reaction conditions, MA formed by the dehydration of ML quickly hydrolyzes to give AA and methanol. Hence, higher selectivity of AA generally depends on the effective and controlled dehydration/hydrolysis reactions. The reversible reaction 2 (**Scheme 2**) i.e. esterification of AA with methanol could also give back MA and this transformation should be prevented or slowed down. Esterification depends on the physicochemical properties of the catalyst system and the operating reaction conditions. Decomposition of ML to form propionic acid, acetaldehyde, carbon monoxide and hydrogen is also to be suppressed. In this respect, we suggest that the proper regulation of the acid–base strength of the composite catalyst is needed, which would improve ML dehydration activity by suppressing the unwanted side reactions. The decreases in acidity and basicity values (**Table 1**), together with the disappearance of TPD peaks of the relatively strong or weak acidic and basic sites in the

Main reactions (Dehydration of ML and hydrolysis of MA)



Side reactions (Decomposition of ML)



Scheme 2. ML conversion and its products.

Table 3Effect of temperature on the dehydration of methyl lactate (ML) using $\text{Ca}_3(\text{PO}_4)_2\text{-Ca}_2(\text{P}_2\text{O}_7)$ [50–50 wt%].

Temperature (°C)	Conv. (%)	Product selectivity (%)				
		Acrylic acid	Methyl acrylate	Acetal-dehyde	Propionic acid	Others ^a
350	30	78	3	13	4	2
370	66	77	4	14	3	2
390	91	75	5	14	4	2
400	95	71	6	16	5	2

Reaction conditions: ML feedstock: 50% in water, ML flow rate: 2.1 ml h⁻¹, LHSV = 0.175, N₂ flow rate: 15 ml min⁻¹, catalyst: 6 ml (4.0 g), TOS: 27 h, (663 K).^a Others contain 0.5–2% of carbon monoxide which are roughly proportional to acetaldehyde formations and the rest are methoxy methyl propionate, acetol, D-lactide and hydrogen.**Table 4**Methyl lactate (ML) conversions using $\text{Ca}_3(\text{PO}_4)_2\text{-Ca}_2(\text{P}_2\text{O}_7)$ [50:50 wt%] composite catalyst at different LHSV and 390 °C.

LHSV (h ⁻¹)	Conv. (%)	Product selectivity (%)				
		Acrylic acid	Methyl acrylate	Acetaldehyde	Propionic acid	Others ^a
0.150	95	72	7	16	3	2
0.175	91	75	5	14	4	2
0.200	79	76	5	13	4	2
0.225	70	77	5	13	4	2

Reaction conditions: ML feedstock: 50% in water, ML flow rate: 2.1 ml h⁻¹, catalyst: 6 ml (4.0 g), TOS: 27 h, temp. = 390 °C.^a Others contain 0.5–2% of carbon monoxide which are roughly proportional to acetaldehyde formations and the rest are methoxy methyl propionate, acetol, D-lactide and hydrogen.**Table 5**Different substrates conversions using $\text{Ca}_3(\text{PO}_4)_2\text{-Ca}_2(\text{P}_2\text{O}_7)$ [50:50 wt%] composite catalyst at 390 °C.

Substrate	Conv. (%)	Product selectivity (%)				
		Acrylic acid	Alkyl acrylate	Acetaldehyde	Propionic acid	Others ^a
EL	57	79	5 (EA)	13	2	1
ML	91	75	5(MA)	14	4	2
LA	100	54	0	14	14	18

Reaction conditions: substrate feed: 50% in water, feed flow rate: 2.1 ml h⁻¹, catalyst: 6 ml (4.0 g), TOS: 27 h.^a Others contain 0.5–2% of carbon monoxide which are roughly proportional to acetaldehyde formations and the rest are methoxy methyl propionate, acetol, D-lactide and hydrogen.

$\text{Ca}_3(\text{PO}_4)_2\text{-Ca}_2(\text{P}_2\text{O}_7)$ [50:50 wt%] composite catalyst, may explain the modulation of the catalytic activity and product selectivity in the cooperative fashion.

The effect of reaction temperature on $\text{Ca}_3(\text{PO}_4)_2\text{-Ca}_2(\text{P}_2\text{O}_7)$ [50:50 wt%] catalyst performance was studied in the ML conversion. The results are presented in Table 3. Keeping other variables the same as in Table 2 data, we varied the reaction temperature between 350 and 400 °C. It was found that the most suitable reaction temperature is 390 °C, which gave the highest selectivity for AA (75%) and MA (5%) at optimum ML conversion (91%). At reaction temperatures above 390 °C, the ML conversion is increased with a drop in selectivity of AA (71%).

The effect of LHSV on the activity of ML conversion and product selectivity was also investigated using the $\text{Ca}_3(\text{PO}_4)_2\text{-Ca}_2(\text{P}_2\text{O}_7)$ [50:50 wt%] while maintaining the reaction conditions as [ML: 50% in water, flow rate: 2.1 ml h⁻¹, LHSV = 0.150–0.225 h⁻¹, N₂ flow rate: 15 ml min⁻¹, catalyst: 6 ml (4 g), TOS: 27 h, temp.: 390 °C] by varying the ML flow rates (LHSV) in the range 0.150–0.225 h⁻¹. The results are presented in Table 4. With increase in LHSV, the ML conversion is decreased from 95 to 70%, while selectivities for AA increased from 72 to 77%, showing the marginal influence.

When different substrates like EL and LA were tested in place of ML (Table 5) with $\text{Ca}_3(\text{PO}_4)_2\text{-Ca}_2(\text{P}_2\text{O}_7)$ [50:50 wt%] under the same reaction conditions [substrate: 50% in water, flow rate: 2.1 ml h⁻¹, LHSV = 0.175 h⁻¹, N₂ flow rate: 15 ml min⁻¹, catalyst: 6 ml (4 g), TOS: 27 h, temp.: 390 °C], it was found that substrate conversions increased in the order of LA > ML > EL. However, the product selectivity increased in the reverse way. The highest AA selectivity of 79% for EL was found, which was followed by ML and LA substrates. Based on the results presented in Table 5, we propose that ML is the

proper substrate to get higher selectivities for AA and MA compared to other substrates.

4. Conclusion

The new $\text{Ca}_3(\text{PO}_4)_2\text{-Ca}_2(\text{P}_2\text{O}_7)$ composite catalyst system was found to be very effective for ML conversion to AA and MA. The composition variation in $\text{Ca}_3(\text{PO}_4)_2\text{-Ca}_2(\text{P}_2\text{O}_7)$ composite catalyst systems revealed the existence of an optimum catalyst composition of 50:50 wt% for the efficient conversion of ML and selective formation of AA and MA. The high catalytic activity of the 50:50 wt% $\text{Ca}_3(\text{PO}_4)_2\text{-Ca}_2(\text{P}_2\text{O}_7)$ composite catalyst was attributed to the existence of moderate acid–base strength regulated through surface properties of $\text{Ca}_3(\text{PO}_4)_2$ and $\text{Ca}_2(\text{P}_2\text{O}_7)$ at 500 °C calcination.

Acknowledgements

This work was supported by Ministry of Knowledge and Economy (MKE) for the program of “Synthesis and Conversion of C3 Platform Chemicals from Biomass (TS-091-49)” and KRICT for Institutional Research Program (KK-1001-B0). Dr. Shiva B. Halligudi acknowledges KOFST for awarding a Brain Pool Fellowship to work at KRICT, Daejeon.

References

- [1] J. van Haveren, E.L. Scott, J. Sanders, *Biopr* 2 (2007) 41–57.
- [2] H. Danner, M. Ürmös, M. Gartner, R. Braun, *Appl. Biochem. Biotechnol.* 70–72 (1) (1998) 887–894.
- [3] J. Young, E. Griffin, J. Russell, *Biomass* 10 (1986) 9–25.

- [4] P.J. de Wild, H. den Uil, J.H. Reith, J.H.A. Kiel, H.J. Heeres, *J. Anal. Appl. Pyrol.* 85 (2009) 124–133.
- [5] X. Tong, Y. Ma, Y. Li, *Appl. Catal. A: Gen.* 385 (2010) 1–13.
- [6] A.V. Bridgwater, *Catal. Today* 29 (1996) 285–295.
- [7] E.F. Iliopoulou, E.V. Antonakou, S.A. Karakoulia, I.A. Vasalos, A.A. Lappas, K.S. Triantafyllidis, *Chem. Eng. J.* 134 (2007) 51–57.
- [8] L.E. Manzer, *Appl. Catal. A: Gen.* 272 (2004) 249–256.
- [9] M.F. Patrick, P. Champagne, M.F. Cunningham, R.A. Whitney, *Bioresour. Technol.* 101 (2010) 8915–9408.
- [10] L.F. Liotta, M. Gruttadauria, G.D. Carlo, G. Perrini, V. Librando, *J. Hazard. Mater.* 162 (2009) 588–606.
- [11] X. Xu, J. Lin, P. Cen, *Chin. J. Chem. Eng.* 4 (2006) 419–427.
- [12] J.M. Lee, D.W. Hwang, Y.K. Hwang, S.B. Halligudi, J.-S. Chang, Y.H. Han, *Catal. Commun.* 11 (2010) 1176–1180.
- [13] G.C. Gunter, D.J. Miller, J.E. Jackson, *J. Catal.* 148 (1994) 252–260.
- [14] G.C. Gunter, R.H. Langford, R.H.J.E. Jackson, D.J. Miller, *Ind. Eng. Chem. Res.* 34 (1995) 974–980.
- [15] S.T. Man, R. Craciun, D.J. Miller, J.E. Jackson, *Ind. Eng. Chem. Res.* 37 (1998) 2360–2366.
- [16] F.S. Hai, C.H. Yao, W. Yang, H. Huang, *Chin. Chem. Lett.* 18 (2007) 476–478.
- [17] H. Wang, D. Yu, P. Sun, J. Yan, Y. Wang, H. Huang, *Catal. Commun.* 9 (2008) 1799–1803.
- [18] P. Sun, D. Yu, K. Fu, M. Gu, Y. Wang, H. Huang, *Catal. Commun.* 10 (2009) 1345–1351.
- [19] Z. Zhiqiang, Q. Yixin, W. Shui, W. Jidong, *Ind. Eng. Chem. Res.* 48 (2009) 9083–9089.
- [20] E.D. Eanes, *Calc. Tiss Res.* 5 (1970) 135–145.
- [21] J. Zhang, J. Lin, X. Xu, P. Cen, *Chin. J. Chem. Eng.* 16 (2008) 263–269.